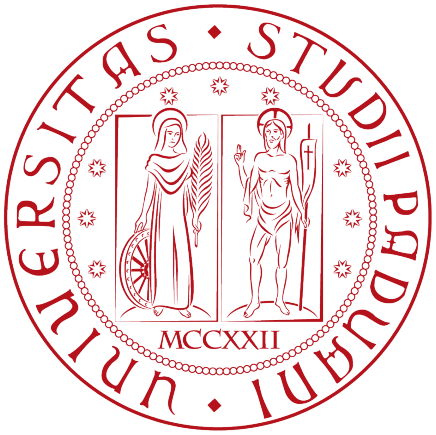

UNIVERSITÀ DEGLI STUDI DI PADOVA

DEPARTMENT OF INFORMATION ENGINEERING

BACHELOR DEGREE IN INGEGNERIA DELL'INFORMAZIONE

CONTROL OF A CARRIER ROCKET

FEDERICO SAPORITI

2000264

SUPERVISOR: PROF. MARIA ELENA VALCHER

Academic Year 2023/2024

Graduation Date: 27 September 2024

I extend my heartfelt gratitude to Professor Elena Valcher
for the considerable time she has devoted to me
and the substantial assistance she has provided
in the composition of this thesis.
I would also like to express my sincere thanks to all those who have
supported me throughout this challenging academic journey:
my family and my dearest friends,
who believed in me from the very beginning.

Abstract

EN:
This thesis focuses on the modelling and control of the planar dynamics of the Ariane V launcher. The study designs a control system that allows the entire system to meet specified performance criteria. In order to evaluate the performance of both open-loop and closed-loop systems under a variety of conditions, including the presence of disturbances, Simulink simulations have been employed. The results demonstrate the effectiveness of the proposed controller in maintaining the stability around the desired trajectory of the rocket.

IT:
La presente tesi è incentrata sulla modellazione e sul controllo della dinamica planare del razzo vettore Ariane V: viene progettato un sistema di controllo che consente all'intero sistema di soddisfare degli specifici criteri di prestazione. Per valutare le prestazioni del sistema ad anello aperto e ad anello chiuso in diverse condizioni operative, compresa la presenza di vari tipi di disturbi, sono state utilizzate simulazioni effettuate tramite Simulink. I risultati dimostrano l'efficacia del controllore proposto nel mantenere la stabilità attorno alla traiettoria desiderata del razzo.

Contents

Introduction

The goal of the thesis is to model and control the planar dynamics of a carrier rocket, Ariane V, orbiting the earth.

After developing a simplified model of the rocket planar dynamics, the thesis aims to explore the possibility of achieving asymptotic stability using a purely proportional controller.
Subsequently, the goal is to design a controller that ensures the stability of the rocket, making it capable of following a specific and constant desired trajectory. The controlled system should also meet specific performance criteria and effectively reject both high and low-frequency disturbances.

Brief Description of Ariane V

Ariane V is widely recognized as a leading European heavy-lift launch vehicle, with its primary mission focused on deploying payloads into geostationary transfer orbit (GTO), geostationary orbit (GEO), and a variety of other orbital trajectories.

Developed by the European Space Agency (ESA) and operated by Arianespace, Ariane V represents one of the world most reliable and extensively utilized launch platforms. Its missions comprehend telecommunications, scientific exploration and Earth observation.

The carrier rocket Ariane V, alongside Soyuz and Vega, played a pivotal

role in ensuring Europe's autonomous access to space.

The maiden launch of Ariane V remains ingrained in history as one of the most costly software errors ever encountered, resulting in a catastrophic failure. Approximately 40 seconds after liftoff, the rocket lost control due to a software malfunction, leading to its destruction. The incident resulted in the loss of four satellites, valued approximately 300 million euros.

Despite this setback, Ariane V has emerged as one of the most reliable launch vehicles, boasting 112 successful missions out of 117 flights, equating a success rate of 95.7%. This success rate, primarily evaluated over its extensive operational history, underscores the rocket reliability, particularly considering its early developmental challenges.

For those reasons, Ariane V has been chosen for some of Europe's most critical missions. Notable missions include the launch of the Rosetta spacecraft in 2004, aimed at the comet 67P/Churyumov–Gerasimenko. Additionally, the ATV cargo capsule, launched with Ariane V on five occasions to resupply and conduct experiments at the International Space Station (ISS), stands as another significant payload. The ATV, one of the largest cargo capsules ever deployed at the ISS, also contributed to the development of the Orion spacecraft service module.

After over 25 years of space launches, Europe's premier launch vehicle, Ariane V, has been officially retired on July 5th, 2023, when Ariane V was launched carrying two telecommunication satellites: the German Heinrich-Hertz-Satellite and the French SYRACUSE 4B, with a combined payload of 7680 kg.

Chapter 1

Modeling

Controlling a carrier rocket means manipulating its movement through mechanical means to achieve the intended path and orientation.
For instance, the attitude (orientation in space) of a rocket is crucial. As shown in Fig. 1.1, its orientation is controlled by rotations around three mutually perpendicular axes: roll, pitch, and yaw.

- The roll axis, x, aligns with the rocket forward motion. Rotations around this axis are measured by the roll angle.
- The z-axis points directly towards Earth.
- The remaining axis, y, is perpendicular to the rocket orbital plane or trajectory.

1.1 Differential Equations and Parameters

The modelization of the aircraft as a rigid body would lead to a set of nonlinear differential equations. In order to derive a linear model we have to introduce some approximations.
The flight is considered to be in steady state, rectilinear with constant velocity and altitude and, finally, we need to introduce an approximation on the structure of the wings, which are considered flat.

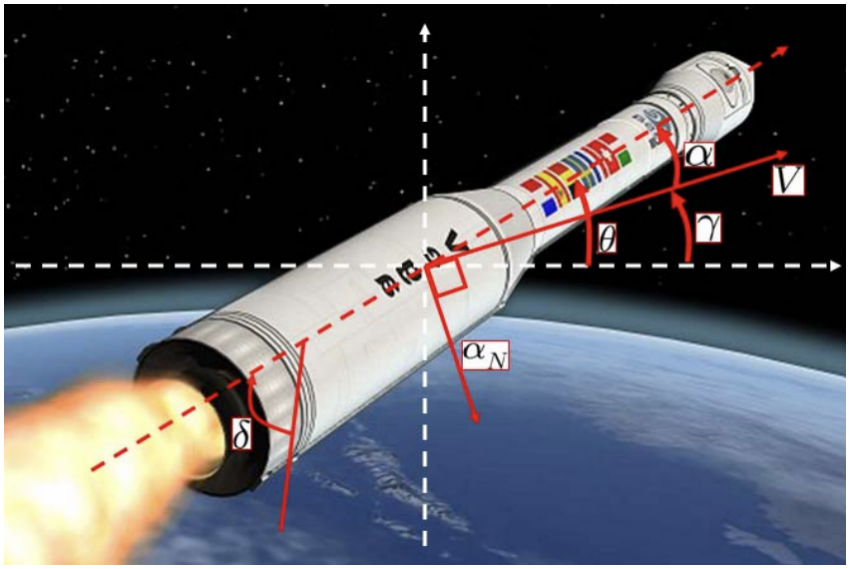

Figure 1.1: Ariane V

These assumptions allow us to obtain the following mathematical model of the linearized planar dynamics of the rocket:

$$\begin{cases} \dot{\alpha} = q + \dfrac{Z_\alpha}{V}\alpha + \dfrac{Z_f}{V}f & \text{(1.1a)} \\ \dot{q} = M_\alpha \alpha + M_f f & \text{(1.1b)} \end{cases}$$

where:

- θ is the pitch angle
- $q = \dot{\theta}$
- α is the angle of attack of the rocket (the angle at which the rocket is tilted with respect to the airstream)
- $V = 416.6 + \beta\,[m/s]$ is the velocity of the rocket
- f is the angular position of the control flap
  - $Z_\alpha = -1390\,[m/s^2]$
  - $Z_f = -371.6\,[m/s^2]$

- $M_\alpha = -248\,[rad/s]$
- $M_f = -622\,[rad/s]$

The provided linearized equations can be interpreted as follows:

Equation for the angle of attack (α)

$$\dot{\alpha} = q + \frac{Z_\alpha}{V}\alpha + \frac{Z_f}{V}f$$

- q is the pitch rate.
- $\frac{Z_\alpha}{V}\alpha$ is the linear contribution of the angle of attack α to the variation of the angle of attack.
- $\frac{Z_f}{V}f$ is the contribution of the control surfaces to the variation of the angle of attack.

Equation for the pitch rate (q)

$$\dot{q} = M_\alpha\alpha + M_f f$$

- $M_\alpha\alpha$ is the contribution of the angle of attack α to the variation of the pitch rate.
- $M_f f$ is the contribution of the control surfaces to the variation of the pitch rate.

1.2 State Space Model

In order to describe the previous system by means of a state space model, we first introduce the state vector $X = (\alpha, q)^T$. We assume as input the angular position of the control flap f, and as output measurement the signal $\alpha_N = -V\dot{\gamma}$, where $\gamma = \theta - \alpha$ is the angle of the flight path.

By deriving $\dot{\gamma} = \dot{\theta} - \dot{\alpha}$, we obtain $\alpha_N = -V\dot{\gamma} = V\dot{\alpha} - V\,q$.
We can use equation (1.1a) to obtain:

$$\alpha_N = -V\dot{\gamma} = V\dot{\alpha} - V\,q = Z_\alpha\,\alpha + Z_f\,f \tag{1.2}$$

It is immediate to deduce that the state space form of the system is:

$$\begin{cases} \dot{X} = \begin{bmatrix} \frac{Z_\alpha}{V} & 1 \\ M_\alpha & 0 \end{bmatrix} X + \begin{bmatrix} \frac{Z_f}{V} \\ M_f \end{bmatrix} f & \text{(1.3a)} \\ \alpha_N = \begin{bmatrix} Z_\alpha & 0 \end{bmatrix} X + \begin{bmatrix} Z_f \end{bmatrix} f & \text{(1.3b)} \end{cases}$$

From now on we will refer to the above equations with the typical matrix notation:

$$\begin{cases} \dot{X} = FX + Gf & \text{(1.4a)} \\ \alpha_N = HX + Jf & \text{(1.4b)} \end{cases}$$

Where:

$$F = \begin{bmatrix} \frac{Z_\alpha}{V} & 1 \\ M_\alpha & 0 \end{bmatrix}; G = \begin{bmatrix} \frac{Z_f}{V} \\ M_f \end{bmatrix};$$
$$H = \begin{bmatrix} Z_\alpha & 0 \end{bmatrix}; J = \begin{bmatrix} Z_f \end{bmatrix}.$$

1.3 Transfer Function

Since the system includes the nonzero term $J = Z_f$, the system is not strictly proper, and therefore the transfer function $G(s) = H(sI - F)^{-1}G + J$ has null relative degree.
To calculate the transfer function, we begin by calculating the matrix $(sI - F)^{-1}$:

$$(sI - F)^{-1} = \frac{1}{s(s - \frac{Z_\alpha}{V}) - M_\alpha} \begin{pmatrix} s & 1 \\ M_\alpha & s - \frac{Z_\alpha}{V} \end{pmatrix}$$

then we obtain:

$$G(s) = \frac{Z_f s^2 + Z_\alpha M_f - Z_f M_\alpha}{s^2 - \frac{Z_\alpha}{V} s - M_\alpha} \tag{1.5}$$

And, after substituting the numerical values, we finally get the transfer function:

$$G(s) = -371.6 \frac{(s - 47.2)(s + 47.2)}{s^2 + 3.329s + 248} \tag{1.6}$$

We can see that the denominator has no sign variations. So, according to Descartes' rule of signs, we can say that the two poles have negative real parts.
On the other hand, in the numerator we have a change of sign and a sign variation, which means that the transfer function has a positive real zero and a negative real zero. In fact, the two complex conjugate poles are:
$s_p = -1.66 \pm 15.65j$ and the two zeros are: $s_z = \pm 47.2$.

1.4 System Stability

By examining the transfer function we can only state that the system is BIBO stable,[1] but in general we cannot determine its asymptotic stability [2] because there may be cancellations of unstable terms between its numerator and denominator.
However, we can avoid further mathematical analysis of the system by noticing that the original system is of second order, which makes it impossible for such cancellations to have occurred, so we can state that the system is asymptotically stable.

[1] For a continuous-time linear time-invariant (LTI) system, a necessary and sufficient condition for BIBO stability is that the impulse response, $h(t)$, is absolutely integrable, i.e., $\int_{-\infty}^{\infty} |h(t)|\, dt = ||h|| \in \mathbb{R}$.

[2] An LTI dynamic system is asymptotically stable if, starting from any initial condition, the system tends to reach the zero state asymptotically.

Chapter 2

Root Locus

Root locus is a technique that allows, given a (proper rational) open-loop transfer function, to plot the path of the closed-loop transfer function poles in the complex plane as the open-loop gain varies in $\mathbb{R}$.

In this chapter, we will build the root locus for both positive and negative feedback systems. We will explore the main characteristics of the root locus and go beyond simply presenting the numerically obtained diagrams.

2.1 Feedback Scheme

We have just seen that the transfer function of our system can be rewritten in the form:

$$G(s) = K_E \frac{n(s)}{d(s)} \tag{2.1}$$

where K_E is the Evans gain, which in our case is negative, and $n(s)$ and $d(s)$ are monic and coprime polynomials belonging to $\mathbb{R}[s]$.

Let us now consider the transfer function of the closed-loop system obtained through negative unitary feedback from $G(s)$, with a proportional controller $C(s) = K$. The Evans gain of the overall open-loop transfer function

is $K_{OL,E} = K_E \cdot K$.
The transfer function of the corresponding closed-loop system is:

$$W(s) = \frac{K_{OL,E}\, n(s)}{d(s) + K_{OL,E}\, n(s)} \tag{2.2}$$

and the resulting block scheme of the system is shown in in Figure 2.1.

Before proceeding with the analysis, we need to make an important observation: as mentioned earlier, the transfer function $G(s)$ has a negative Evans gain, i.e., $K_E \leq 0$.
Therefore, when analyzing the stability of the closed-loop system, as the controller gain K varies, we must keep into account the fact that the open-loop gain is $K_{OL,E} = K \cdot K_E$ and so it will be negative if $K > 0$, and positive if $K < 0$.

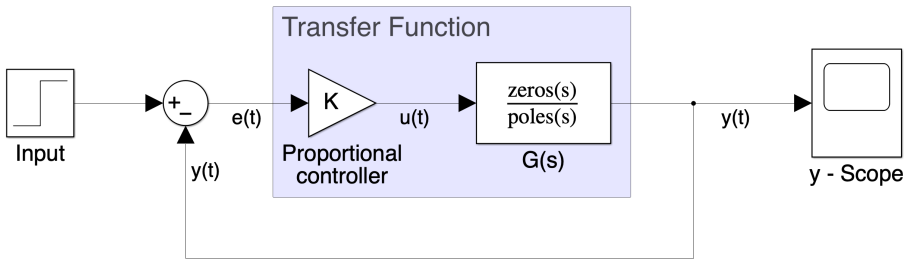

Figure 2.1: Block system scheme with proportional controller

2.2 Positive Root Locus

As we can notice from equation (2.2), knowing that $d(s)$ and $n(s)$ are coprime polynomials, as $K_{OL,E}$ varies in $\mathbb{R}/\{0\}$

$$\{\text{poles of } W(s)\} \equiv \{\text{zeros of } d(s) + K_{OL,E}\, n(s)\}$$

and, by definition, the positive root locus coincides with the set:

$$\{\alpha \in \mathbb{C} \mid \exists\, K_{OL,E} > 0 \mid d(\alpha) + K_{OL,E}\, n(\alpha) = 0\}.$$

Since $G(s)$ is a proper (and not strictly proper) function, the degree of the numerator coincides with the degree of the denominator: this means that the ratio of the numerator to the denominator tends to a (nonzero) constant value as s tends to infinity. Therefore, the locus has no asymptotes as $K_{OL,E}$ goes to infinity. All the root locus branches end in the zeros of $G(s)$.

Multiple points of the locus, i.e. the points where two or more branches of the locus cross each other, can be obtained by solving the multiple point candidate equation:

$$n(s)\,\frac{d}{ds}\,[d(s)] - d(s)\,\frac{d}{ds}\,[n(s)] = 0 \tag{2.3}$$

that results to be:

$$(s^2 - 2228.26)(2s + 3.329) = 2s(s^2 + 3.329s + 248)$$

And, after doing some calculi, we obtain:

$$3.329s^2 + 4951.68s + 7416.5 = 0$$

whose solutions are the two points $\alpha_1 = -1.5$ and $\alpha_2 = -1485.9$.

Those points are candidate multiple points, so we have to verify if they really are: since both α_1 and α_2 are real numbers different from 0 and they are not double-zeros or double-poles of $G(s)$, this allows us to say that they

are both multiple points of the locus.

Now, to understand if they belong to the direct or inverse root locus we have to evaluate if $K_\alpha = -d(\alpha)/n(\alpha)$ is positive or negative.
It turns out that $K_{\alpha_1} > 0$ and hence α_1 belongs to the direct locus, while $K_{\alpha_2} < 0$, thus implying that α_2 belongs to the inverse locus. We now have all the information to plot the positive root locus.

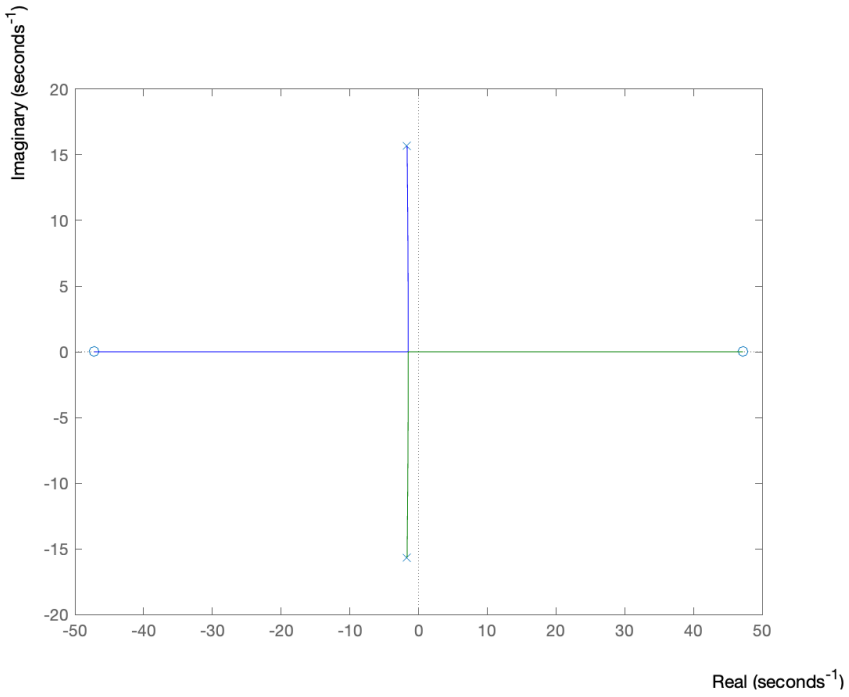

Figure 2.2: Positive root locus

The portion of the real axis that belongs to the direct locus[1] is the one between the two zeros. The system becomes unstable values of $K_{OL,E}$, due to the branch that tends to the non-minimum phase zero.

It is immediate to see from the locus, without making any calculations, that for low and positive values of $K_{OL,E}$ BIBO-stability is granted, because

[1]Direct locus is another way to call the positive locus.

both branches are in the negative real part of the complex plane. However, for values of $K_{OL,E}$ higher than the value that corresponds to the crossing of the origin by a branch towards the positive half-plane, we no longer have stability.

We can now proceed to explicitly calculate that value of $K_{OL,E}$ for which the branch passes from the negative to the positive half-plane along the real axis.
We must impose the condition

$$d(0) + K_{OL,E}\, n(0) = 0$$

thus obtaining

$$K_{OL,E} = \frac{248}{(47.2)^2} = 0.1113$$

and so we obtain

$$K = K_{OL,E}/K_E = -0.0003.$$

K is negative, as expected from the initial premise and it is a very small value, as we mentioned before.
From the direct locus we therefore conclude that stability is satisfied for values of the controller gain $K \in (-0.0003, 0)$.

2.3 Negative Root Locus

The inverse root locus, shown in Figure 2.3, is obtained for positive values of the gain K, as mentioned before. The portions of the real axis that belong to the inverse locus are complementary to those that belong to the direct locus, since the entire real axis is contained in the union of the direct and inverse locus.

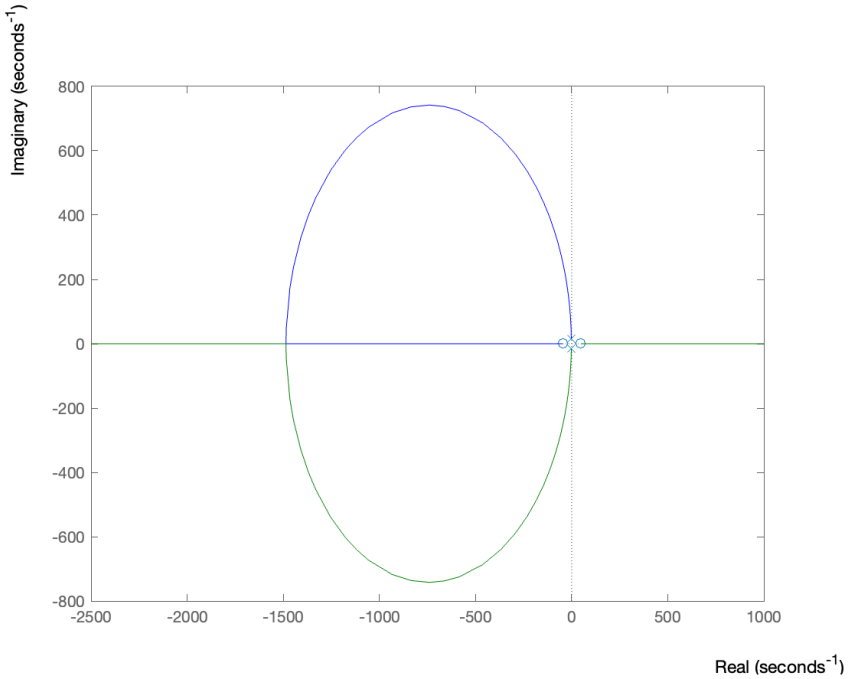

Figure 2.3: Negative root locus

We can see in Figure 2.3 and 2.4 that the green branch, which starts from the pole $s_p = 1.66 - 15.65j$, for $K_{OL,E} \to 0^-$, terminates in the real zero $s_z = +47.2$, without passing through the origin.

To determine the value of $K_{OL,E}$ for which the green branch approaches $-\infty$ along the real axis, thereby obtaining the stability margin value for $K_{OL,E}$, we can proceed as follows: since $n(s)$ and $d(s)$ are monic and coprime polynomials, the green branch tends towards $-\infty$ when $d(s) + K_{OL,E}\, n(s)$ has a degree lower than $\deg d(s) = \deg n(s)$.

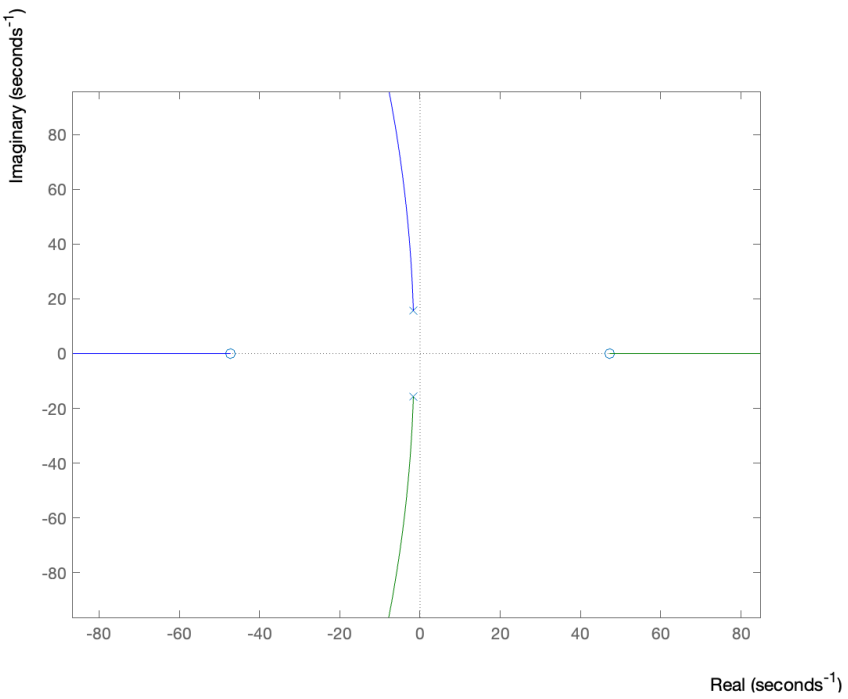

Figure 2.4: Zoom on the origin of the negative root locus

This trivially occurs if and only if $K_{OL,E} = -1$.

We can now conclude that we must have:

$$0 \geq K_{OL,E} > -1$$

and, knowing that $K_{OL,E} = K \cdot K_E$ from the negative locus, we therefore conclude that BIBO-stability is satisfied for:

$$0 \leq K < 0.0027$$

2.4 Stability Analysis Conclusions

We can distinguish 3 intervals for the values of the gain K:

- $K < -0.0003$
- $-0.0003 < K < 0.0027$
- $K > 0.0027$

For $K < -0.0003$, the coefficient of s^2 is negative, while the other 2 are positive $(-++)$, therefore there is a sign change in the numerator of polynomial 2.2, and therefore the polynomial has a root with positive real part.

For $-0.0003 < K < 0.0027$, we have no sign changes but only sign permanence, and therefore the system is BIBO-stable.

For $K > 0.0027$, the situation is similar to the first one as there is only one sign change $(++-)$ and therefore the polynomial has a root with positive real part.

In conclusion, BIBO-stability is achieved if and only if $-0.0003 < K < 0.0027$, as the closed-loop transfer function $W(s)$ has all poles with negative real part, which means that all elementary modes of the impulse response $w(t)$ are convergent and so the system always responds with a (forced) bounded output to any bounded input.

Chapter 3

Stability Analysis with Nyquist Criterion

In this chapter we will discuss, using the Nyquist criterion, whether it is possible to make the system BIBO-stable with a purely proportional controller and a unitary negative feedback control scheme. As one can notice, this is exactly what was done before with the root locus, but everything we are going to discuss in this chapter will be useful for the controller design that we will be doing in the next chapter.

3.1 Brief description of the Nyquist Criterion

As ω varies continuously over the interval $(0, +\infty)$, the frequency response $G(j\omega)$ describes a curve in the complex plane. This curve is generally continuous, with at most a finite number of discontinuities, since $G(s)$ is a rational function.
This curve, parameterized in ω and oriented in the direction of increasing ω, is called Nyquist diagram.
There are two ways to plot the Nyquist diagram:

1. The analytical method consists of the analytical study of the real and imaginary parts of $G(j\omega)$, $Re[G(j\omega)]$ and $Im[G(j\omega)]$, for ω varying

in the interval $(0, +\infty)$. By combining the two curves, the complete Nyquist plot is obtained.

2. The method based on the Bode diagram, which consists of first drawing the Bode diagram and then obtaining the Nyquist diagram by looking at how the modulus and phase vary as ω varies.

We are going to use the second method.

The Nyquist criterion is a method used to study the BIBO-stability of a closed-loop system, with a proper rational transfer function $W(s)$, obtained from a proper rational transfer function $\tilde{G}(s)$ by negative unitary feedback. The Nyquist criterion assumes that $G(s)$ is known only through its Nyquist plot.
The Nyquist criterion assumes the knowledge of the following information:

1. the Nyquist diagram of $\tilde{G}(s)$, for every $\omega \in \mathbb{R}$ (if we know the Nyquist diagram of $\tilde{G}(j\omega)$ for $\omega \geq 0$, we can easily find the diagram for $\omega \leq 0$ by exploiting the Hermitian simmetry);

2. the number of poles with positive real part of $\tilde{G}(s)$.

Let us now assume that $\tilde{G}(s) = G(s)$.
We will use the Nyquist Criterion by introducing two conditions, which in our case won't be restrictive:

C1 The Nyquist diagram of $G(j\omega)$ must remain bounded for every $\omega \in \mathbb{R}$;

C2 The Nyquist diagram does not pass through the critical point $-1 + j0$.

Let us define N as the number of turns that the Nyquist diagram makes around the critical point $-1 + j0$ as $\omega : -\infty \to +\infty$, counted with a positive sign if they are described clockwise and negative otherwise.
The Nyquist criterion states that the following relationship then holds:

$$N = n_G^+ - n_W^+, \tag{3.1}$$

where n_G^+ is the number of poles with positive real part of $G(s)$ and n_W^+ is the number of poles with positive real part of $W(s)$.
It is then immediate to notice that $W(s)$ is BIBO stable if and only if $N = n_G^+$. Moreover, if $G(s)$ is BIBO stable ($n_G^+ = 0$), then $W(s)$ is BIBO stable if and only if $N = 0$.

3.2 Nyquist Diagram

Let's begin by drawing the Bode plot: first we need to rewrite $G(s)$ in Bode form:

$$G(s) = 3338.17 \frac{\left(1 - \frac{s}{47.2}\right)\left(1 + \frac{s}{47.2}\right)}{1 + 2\,\frac{1.6645}{\sqrt{248}}\frac{s}{\sqrt{248}} + \frac{s^2}{248}} \tag{3.2}$$

The Bode gain in dB, which in our case is the modulus in dB of $G(j\omega)$ for $\omega = 0$, is:

$$|W(j0)|_{dB} = 20\,log_{10}(3338.17) = 70.47\,dB$$

Now we have all the information to plot the Bode diagram:

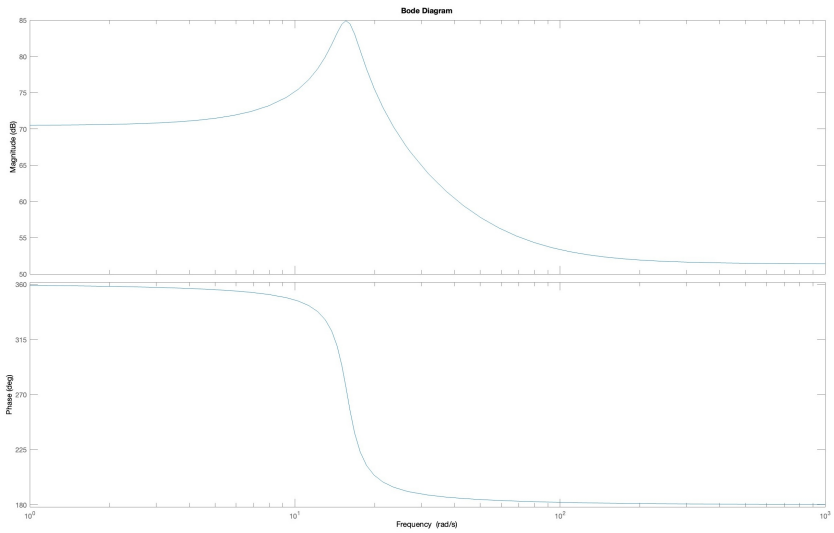

Figure 3.1: Bode plot of $G(s)$

In the amplitude diagram, the peak is present due to the pair of conjugated complex poles, with damping coefficient:

$$\xi = \frac{1.6645}{\sqrt{248}} = 0.106$$

In the phase diagram, thanks to the fact that the damping is rather small, the descent around $\omega = \sqrt{248} \approx 15.75\,[rad/s]$ is rather rapid.

Now drawing the Nyquist plot is immediate: the Bode diagram and the Nyquist diagram provide equivalent information about the frequency response $G(j\omega)$ of a system. In fact, from the Bode diagram of the amplitudes, once its values have been converted from dB into absolute values, it is possible to determine for all ω the quantity $|G(j\omega)|$ and therefore, with reference to the Nyquist diagram, the modulus of the vector from the origin of the plane to the point $G(j\omega)$ of the diagram. From the Bode plot of the phases we can determine the angle that the vector forms with the positive real semi-axis. We are now able to draw the Nyquist plot of the negative unitary feedback system.

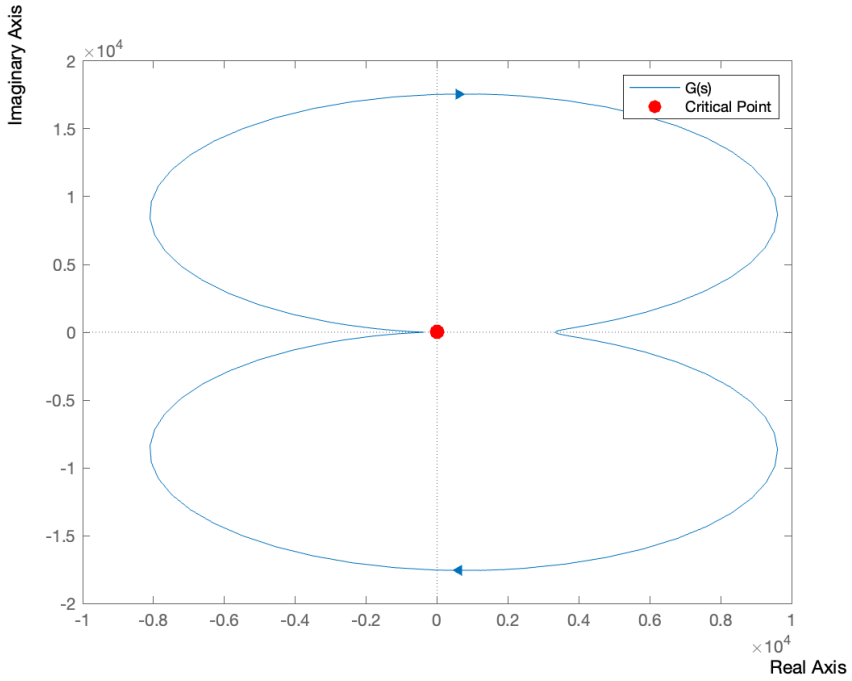

Figure 3.2: Nyquist diagram of $G(s)$

3.3 Conclusions

As expected, the system obtained from $\tilde{G}(s)$ through negative unitary feedback is not stable: we have proven in ch.1.4 that the open-loop system is asymptotically stable (which guarantees BIBO-stability), so we must have $N = 0$ to grant stability of $W(s)$. The diagram surrounds the critical point once clockwise and so we have $N = 1$. This is because for $W(s)$ to be stable, $C(s) = K$ must satisfy $-0.0003 < K < 0.0027$. However, in this chapter, we are considering $K = 1$.

If we want to study the stability of the closed-loop system as K varies it is sufficient to notice that:

$$W(s) = \frac{KG(s)}{1 + KG(s)} = \frac{G(s)}{\frac{1}{K} + G(s)}$$

We can now adapt the previous version of the Nyquist criterion by replacing the fixed critical point $-1 + j0$ with the variable critical point $-\frac{1}{K} + j0$.
In our case it is immediate to notice that, for both positive and negative values of K, as long as they are small enough, the critical point comes out of the curve and therefore stability is granted.

To precisely get these values from Nyquist Criterion we must study it with the analytical method, but it would be quite time-consuming and, since we already got the results we wanted from root locus, we are not going to do so. In the following figure, the values of the intersections between the Nyquist diagram and the real axis are shown, to graphically prove what we just said.

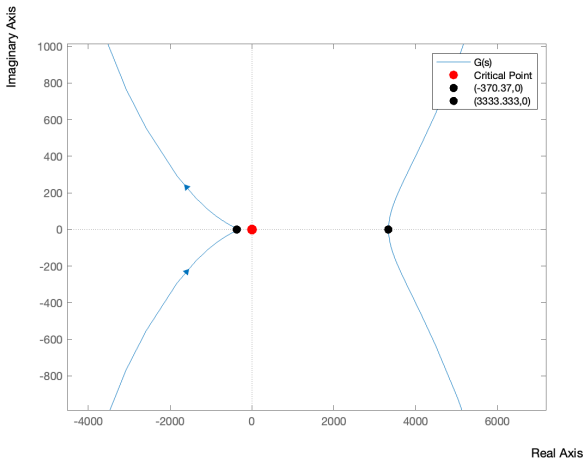

Chapter 4

Control System Design

In this chapter, we will develop a controller to be put in cascade with $G(s)$, followed by a unitary feedback. This controller will stabilize the rocket dynamics and guarantee that the resulting system satisfies some design specifications, which will be presented subsequently.

4.1 Specifications

We want to design a controller $C(s)$ to be put in a cascade with $G(s)$ that guarantees the following specifications:

1. Steady-state error e_{rp} less than $0.03[m/s^2]$ in module for the closed-loop system, corresponding to a unitary step reference for the normal acceleration α_N;

2. Percentage overshoot of the closed-loop system in response to a step input reference $S \leq 9\%$.

3. Attenuation of the closed-loop system equal to 0.01 for measurement disturbances with frequency components $\omega \geq 100\,[rad/s]$;

4. If the closed-loop system presents parametric variations, the sensitivity of the overall system should be lower by a 10 factor than the sensitivity

of the system under nominal conditions, for inputs at frequencies $\omega \leq 0.1\,[rad/s]$.

The controller design will be divided into 2 parts: the controller will be written in the form:

$$C(s) = C_1(s)C_2(s).$$

We can also notice that, in order to satisfy the second specification, it is necessary to analyze the step response in the time domain of the closed-loop system. However, such an analysis would be quite time-consuming. Therefore, in the next paragraph, we will attempt to derive a relationship between the required percentage overshoot and the phase margin of the open-loop system.

4.2 Second specification

Let us assume the system is BIBO-stable and define $\bar{S}$ as the maximum overshoot value:

$$\bar{S} = \left| \frac{y_{max} - \bar{y}}{\bar{y}} \right|,$$

where:

- y_{max} is the maximum value reached by the step response $w_{-1}(t)$;
- $\bar{y}$ is the steady state value of the step response $w_{-1}(t)$;

We begin by recalling the transfer function of the open-loop system (eq.1.6):

$$G(s) = -371.6\frac{(s - 47.2)(s + 47.2)}{s^2 + 3.329s + 248}$$

Our system is a second-order one. Now, we'll approximate the open-chain system $C(s)G(s)$ to another second-order system without zeros since the two poles are dominant[1]: in fact, as shown at the end of ch.1.3, the two complex conjugate poles are: $s_p = -1.66 \pm 15.65j$

[1] If a system has two complex poles (obviously stable), whose real parts are at least ten times smaller in absolute value than any other pole or zero, it is said to have "two dominant poles".

and the two zeros are: $s_z = \pm 47.2$.
The second-order system we are approximating is expressed in the following form:

$$\frac{1}{1 + 2\delta\frac{s}{\omega_n} + \frac{s^2}{w_n^2}} \tag{4.1}$$

We now need to derive the relationship between minimum damping ratio δ and $\bar{S}$.
The step response of a second-order system is determined by the inverse Laplace transformation, resulting in:

$$y(t) = \mathscr{L}^{-1}\left\{\frac{1}{s(1 + 2\delta\frac{s}{\omega_n} + \frac{s^2}{w_n^2})}\right\} = (1 - Ae^{-\delta\omega_n t}sin(\beta t + \phi))\,\delta_{-1}(t) \tag{4.2}$$

where $A = \frac{1}{\sqrt{1-\delta^2}}$ and $\phi = arctan\,\frac{\sqrt{1-\delta^2}}{\delta} = arccos\,\delta$.
In order to find the maximum value of $y(t)$ we have to set the derivative equal to 0:

$$\frac{dy}{dt} = -Ae^{-\delta\omega_n t}\beta cos(\beta t + \phi) + A\delta\omega_n e^{-\delta\omega_n t}\beta sin(\beta t + \phi) = 0 \tag{4.3}$$

simplifying we obtain:

$$\delta\omega_n \sin(\beta t + \phi) - \omega_n\sqrt{1 - \delta^2}\cos(\beta t + \phi) = 0$$

and it is true if and only if:

$$tan(\beta t + \phi) = \frac{\sqrt{1 - \delta^2}}{\delta}$$

and, since $\phi = arctan\,\frac{\sqrt{1-\delta^2}}{\delta}$ we have:

$$\beta t = K\pi, \qquad K \in \mathbb{N},$$

and so we obtain the set of time instants:

$$t_K = \frac{K\pi}{\beta} = \frac{K\pi}{\omega_n\sqrt{1 - \delta^2}} \quad , \quad K \in \mathbb{N}.$$

By substituting these instants into the response we obtain:

$$y(t_K) = 1 - \frac{e^{-\frac{K\pi\delta}{\sqrt{1-\delta^2}}}}{\sqrt{1 - \delta^2}}sin(K\pi + \phi) = 1 - (-1)^K e^{-\frac{K\pi\delta}{\sqrt{1-\delta^2}}} \quad , \quad K \in \mathbb{N} \tag{4.4}$$

and so we have:

$$\bar{S} = y(t_1) - 1 = e^{-\frac{\pi\delta}{\sqrt{1-\delta^2}}}. \tag{4.5}$$

Now we know that at the crossover frequency ω_a of the open-loop system we have:

- $|C(j\omega_a)G(j\omega_a)| = 1$
- $\angle C(j\omega_a)G(j\omega_a) = \phi_a = -\pi + P_m$

Where P_m is the phase margin and it is defined as shown above.
Therefore, given $C(j\omega_a)G(j\omega_a) = e^{j\phi_a}$, we can write:

$$W(j\omega_a) = \frac{e^{j\phi_a}}{1 + e^{j\phi_a}}$$

from which we obtain (recalling the formula for sine bisection: $\sin(\alpha/2) = \pm\sqrt{(1-\cos\alpha)/2}$):

$$|W(j\omega_a)| = \frac{1}{|1 + e^{j\phi_a}|} = \frac{1}{\sqrt{2(1-\cos(P_m))}} = \frac{1}{2\sin(P_m/2)} \tag{4.6}$$

and

$$\angle W(j\omega_a) = \phi_a - arctan\left(\frac{sin(\phi_a)}{1 + cos(\phi_a)}\right) \tag{4.7}$$

To determine the damping of the dominant poles from the Bode diagram of $G(s)$, by comparing 4.1 with 4.6, using the properties of the crossover frequency written on top, we obtain:

$$|W(j\omega_a)| = \frac{1}{2\delta} = \frac{1}{2sin(P_m/2)} \tag{4.8}$$

from which we derive $\delta = \sin(\frac{P_m}{2})$ and, for values of P_m smaller than 70°, we can use the approximate relation (where P_m is expressed in degrees):

$$\delta = \frac{P_m}{2}\frac{\pi}{180} \approx \frac{P_m}{100} \tag{4.9}$$

Now we're almost done: we just need to establish the relationship between P_m and $\bar{S}$.

We can derive the minimum damping δ from eq. (4.5) as:

$$0.09 = \bar{S} = e^{-\frac{\pi\delta}{\sqrt{1-\delta^2}}}$$

thus obtaining

$$\delta \approx 0.6.$$

And now we just need to use the relationship we just derived in eq.(4.9), obtaining:

$$P_m = 100\,\delta = 60^\circ$$

In conclusion, we can state that for our system, the second specification, which requires having an overshoot $S \leq 9\%$, can be translated into the frequency domain by imposing that the open-loop transfer function has a phase margin $P_m \geq 60^\circ$.

4.3 First Proportional Controller

Since the open loop system is BIBO-stable, it is possible to proceed with the design on the Bode diagram.

In order to satisfy the first specification it is necessary, by the final value theorem, that the error transform $E(s)$ of the closed loop system, calculated at $s = 0$ is smaller than or equal to 0.03, that is:

$$\lim_{s\to 0} sE(s)\frac{1}{s}|_{s=0} = \frac{1}{1+KG(s)}|_{s=0} = \frac{1}{1+K\frac{371.6\cdot 2228}{248}} \leq 0.03 \tag{4.10}$$

which imposes a gain value $K \geq 0.009$.
From the stability analysis addressed in Chapter 2, we know that to guarantee BIBO-stability through a simple proportional controller, its gain must fall within the range of $-0.0003 < K < 0.0027$. We therefore understand that, in order to satisfy this condition, we have to choose a gain, for example $K = 0.009$ that will not guarantee BIBO-stability.
There is also another way of solving this problem which would be by incrementing the type of the system by 1 by introducing a pole in zero in the first controller, but this would complicate a lot the process of satisfying the second specification. We will then choose the gain $K = 0.009$ and we will impose BIBO-stability later, with the second controller.

We will now try to see if, with this controller, the fourth specification is satisfied, i.e. $S_{LF}(s) \leq 0.1$ for inputs at frequencies $\omega \leq 0.1\,[rad/s]$.
We are going to impose that the sensitivity function $S_{LF}(j\omega)$ at low frequencies[2] is less than or equal to 0.1:

$$|S_{LF}(j\omega)| = \left|\frac{1}{1+G(j\omega)C_1(j\omega)}\right| \leq 0.1 \tag{4.11}$$

simplifying, we obtain

$$10 \leq |1 + C_1(j\omega)G(j\omega)|$$

and, converting to decibel we obtain:

$$|1 + C_1(j\omega)G(j\omega)|_{dB} \geq 20dB \tag{4.12}$$

[2]More details on $S_{LF}(j\omega)$ are shown in Appendix A

and the fourth specification is automatically satisfied with the gain $K = 0.009$, as shown by the Bode diagram of $C_1(j\omega)G(j\omega)$ obtained corresponding to the proportional controller $C_1(s) = 0.009$, in figure 4.1.

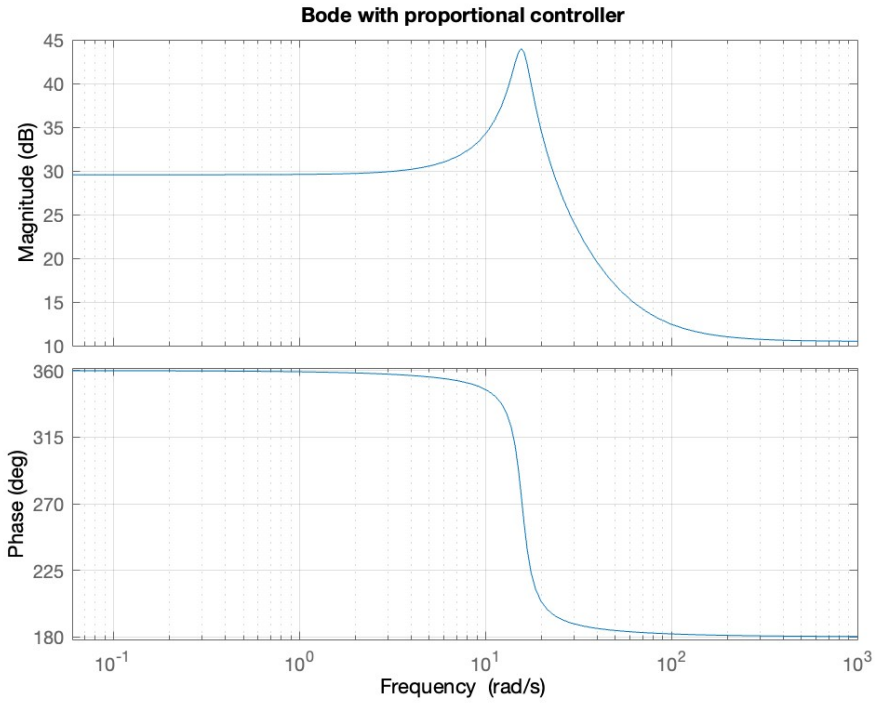

Figure 4.1: Bode diagram with C1

4.4 Second controller

Through the design of the second controller, we will fulfil all the specifications and ensure the BIBO-stability of the system.

We begin by satisfying the third specification: first we must take a look at the closed-loop system with disturbances shown below:

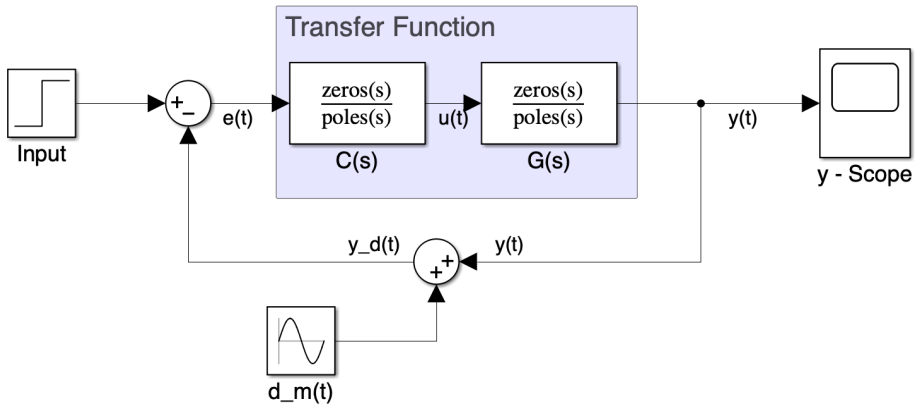

Figure 4.2: closed-loop system with disturbances

The transfer function from the measurement noise to the system output is given by:

$$\left|\frac{Y(j\omega)}{D_m(j\omega)}\right| = \left|\frac{C(j\omega)G(j\omega)}{1+C(j\omega)G(j\omega)}\right| \tag{4.13}$$

which is equal in module to the complementary sensitivity function

$$|\bar{S}_{LF}(j\omega)| = |1 - S_{LF}(j\omega)|$$

According to the specifications, $|\bar{S}_{LF}(j\omega)|$ must be less than or equal to 0.01 for $\omega \geq 100[rad/s]$, which leads us to the following inequality:

$$|C(j\omega)G(j\omega)| \leq \frac{0.01}{0.99} \approx 0.01$$

and, converting to decibel we obtain:

$$|C(j\omega)G(j\omega)| \leq -40\,dB \tag{4.14}$$

It is therefore necessary to decrease the modulus of $C(s)G(s)$ at high frequencies if we want to satisfy the third specification.
In order to do so, we can introduce a pole before the two conjugated complex poles of $G(s)$, but the problem remains as we have to satisfy the second specification, i.e. $P_m \geq 60°$.
We therefore must choose the right frequency at which we want to put this pole.
By looking at the Bode diagram in Figure 4.2, obtained by inserting the first controller in cascade to $G(s)$, we can see that it is sufficient to insert the pole at least a couple of decades before the poles of $G(s)$. If we put a pole, for example in $s_p = -\frac{1}{27} = 0.037$, this should be enough.
Due to the presence of the aforementioned pole, a gain drop is observed at low frequencies, which requires an increase in the controller gain up to $K = 0.0116$ to satisfy the fourth specification.
The controller that satisfies all specifications then results:

$$C(s) = C_1(s) \cdot C_2(s) = 0.009 \cdot \frac{1.28889}{27s+1} = \frac{0.0116}{27s+1}. \tag{4.15}$$

4.4.1 BIBO-stability analysis

With the controller we have designed, the closed-loop transfer function results:

$$W(s) = \frac{C(s)G(s)}{1 + C(s)G(s)} = \frac{-0.1597s^2 + 355.7}{s^3 + 3.206s^2 + 248.1s + 364.9} \tag{4.16}$$

and the Bode diagram of the controlled system is shown in Figure 4.3.
From the Bode diagram we have plotted we can also conclude that the feedback system $W(s)$, obtained with the controller $C(s)$, is BIBO-stable thanks to the Bode criterion, which states that $W(s)$ is BIBO-stable if:

1. $C(s)G(s)$ does not have positive real part poles;
2. the Bode gain of $C(s)G(s) = K_B(G) \cdot K_B(C)$ is positive;
3. the phase margin P_m of $C(s)G(s)$ is positive.

The final structure of the system is shown in Figure 4.4.

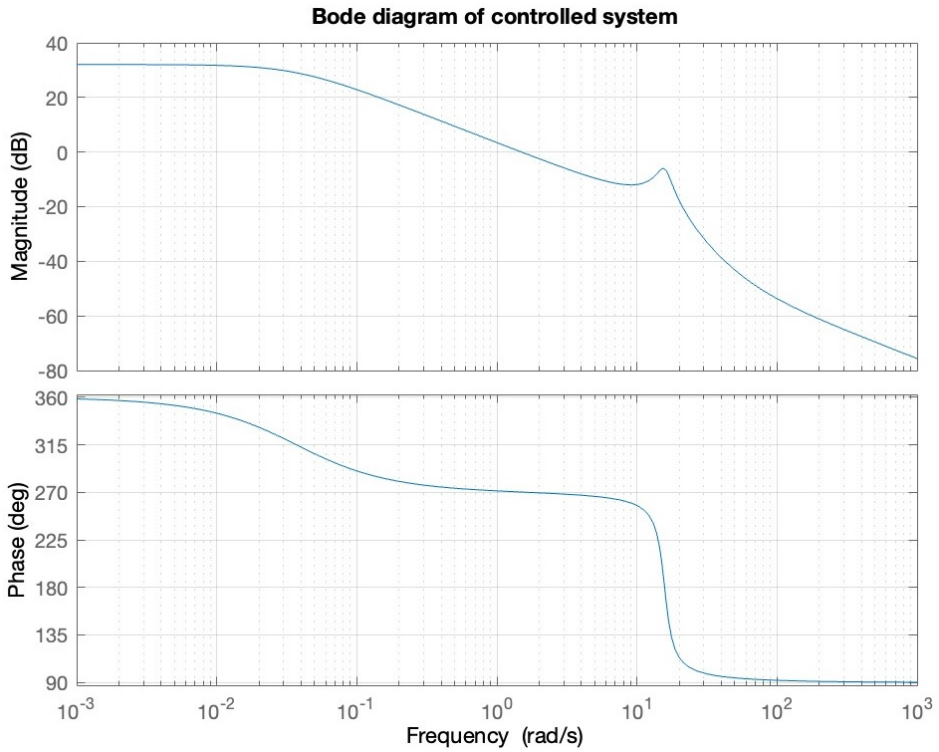

Figure 4.3: Bode diagram of the controlled system

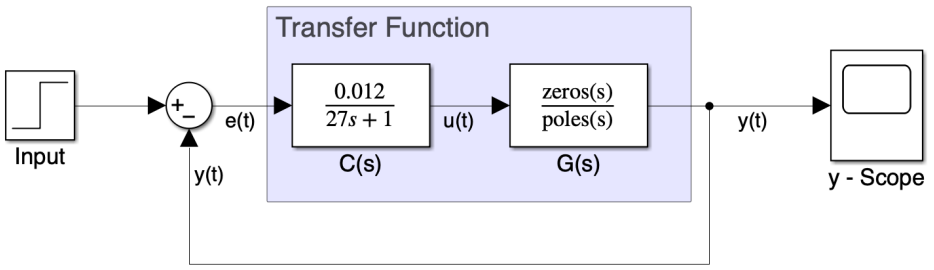

Figure 4.4: Closed-loop controlled system

Chapter 5

Performance analysis

Let us now apply, first to the open-loop system, then to the closed-loop one, a unitary step input signal and observe their forced responses to understand their performance. We will then apply a measurement disturbance as shown in Figure 4.2 and we will observe how the open-loop system responds to disturbances at frequencies higher than $100[rad/s]$ and we will compare the performances with the closed-loop step response.

5.1 Open-Loop System

The step response $y(t)$ of the open-loop system is shown in Figure 5.1.
The regime value of the open-loop step response $y(\infty)$ is obtained by applying the final value theorem to $Y(s) = G(s)\frac{1}{s}$:

$$\lim_{s\to 0} sG(s)\frac{1}{s} = \frac{371.6 \cdot (47.2)^2}{480} \approx 3338 \tag{5.1}$$

while the initial value y(0) is obtained by applying the initial value theorem:

$$\lim_{s\to \infty} sG(s)\frac{1}{s} = K_E = -371.6. \tag{5.2}$$

We can observe that the sign of $y(0)$ and $y(\infty)$ are discordant, giving rise to the characteristic phenomenon of “inversion", also called undershoot, of the step response of non-minimum phase systems.
The system also has two complex conjugate poles whose associated modes have

an exponential decay rate $\lambda = -1.66$, with frequency $\omega = \sqrt{248 - (1.66)^2} = 15.75$. This results in an oscillation pattern with an approximate distance between successive peaks equal to $T = \frac{2\pi}{\omega} \approx 0.4s$. The associated mode of the two conjugated poles is:

$$\gamma(t) = e^{-1.66t} sin(15.75t) \tag{5.3}$$

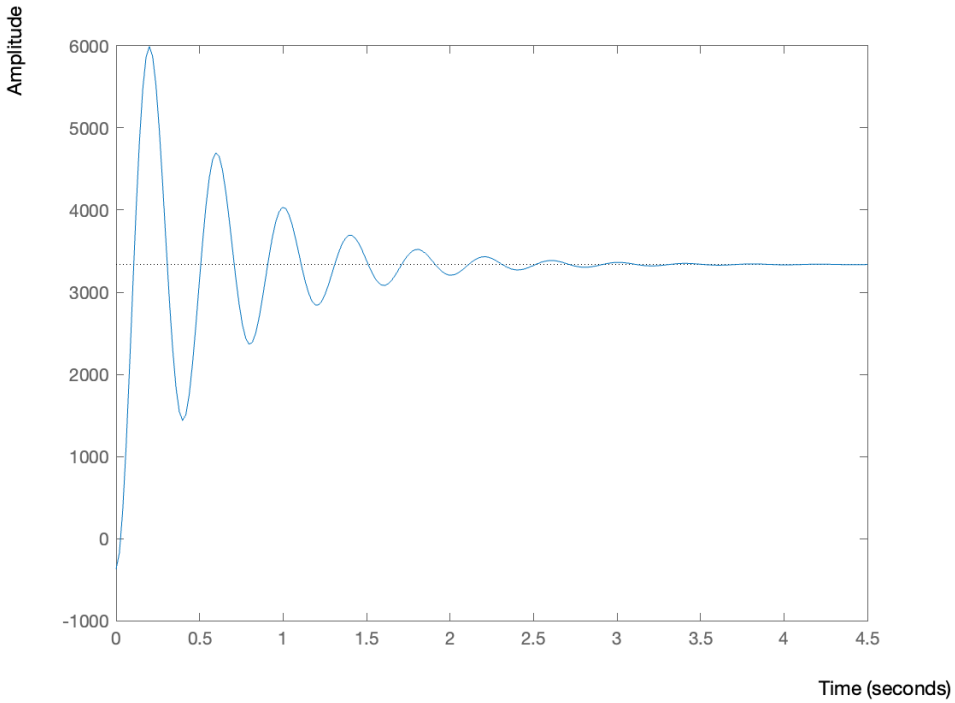

Figure 5.1: Step response of open-loop system

5.2 Closed-Loop System

The step response of the controlled system is shown in Figure 5.2, and corresponds to the inverse transform of the function:

$$Y(s) = \frac{C(s)G(s)}{1 + C(s)G(s)} \frac{1}{s} = \frac{-0.1597s^2 + 355.7}{s^3 + 3.206s^2 + 248.1s + 364.9} \frac{1}{s} \tag{5.4}$$

The closed-loop transfer function has a decreasing exponential mode and an

exponentially modulated sinusoidal mode which are both asymptotically stable.
In particular, the poles of the transfer function are:

$$\begin{cases} p_1 = -0.86 - 15.65j \\ p_2 = -0.86 + 15.65j \\ p_3 = -1.49 \end{cases}$$

thus leading to a transient response with asymptotically stable modes:

$$\begin{cases} \gamma_1(t) = e^{-1.49t} \\ \gamma_2(t) = e^{-0.86t} sin(15.65t). \end{cases}$$

In this case, the presence of non-minimum phase zeros is highlighted by the negative value taken by the derivative $\frac{dy}{dt}$ of the step response when $t \to 0$, in fact:

$$\lim_{s\to\infty} s^2 W(s)\frac{1}{s} = \frac{-4.31}{27} = -0.16, \tag{5.5}$$

while the steady-state value of the step response is obtained by applying the final value theorem and it holds:

$$\lim_{t\to\infty} y(t) = \lim_{s\to 0} sW(s)\frac{1}{s} = \lim_{s\to 0} \frac{-0.1597s^2 + 355.7}{s^3 + 3.206s^2 + 248.1s + 364.9} = \frac{355.7}{364.9} = 0.975. \tag{5.6}$$

After running the MATLAB code shown in Appendix B, the following step response infos are provided:

RiseTime[1]: 1.3096 [s]
SettlingTime (5%) : 2.1667 [s]
Overshoot: 0.0916%
Undershoot: 0.2647%
Peak: 0.9757
PeakTime: 4.3103 [s]

[1]The default definition of rise time is the time it takes for the response to go from 10% to 90% of the way from $y_{init} = 0$ to y_{final}

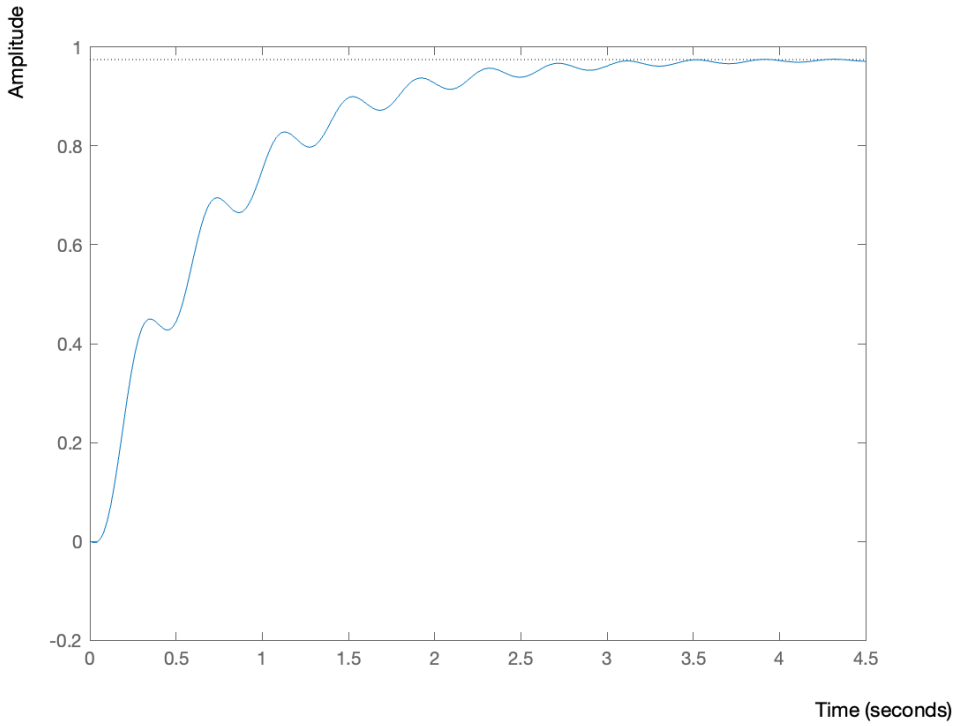

Figure 5.2: Step response of the closed-loop system

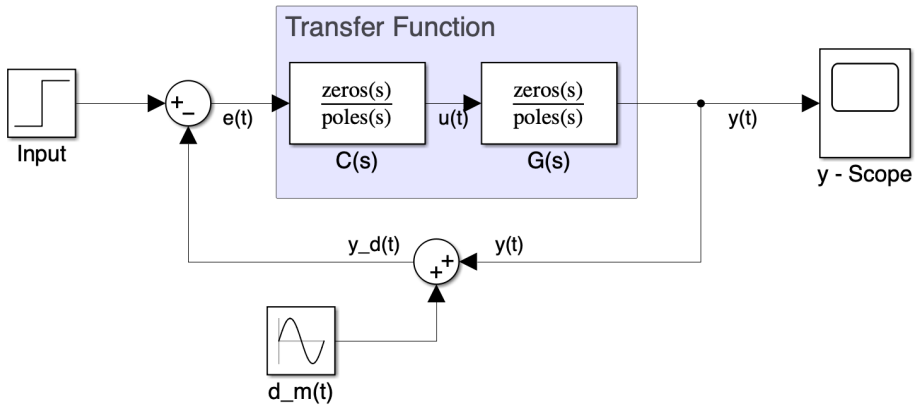

Figure 5.3: Closed-loop system with disturbances

5.3 Performance analysis with measurement disturbance

We aim to evaluate the step response of the system with measurement disturbance as the frequency of the disturbance $\omega > 100$ [rad/s] varies. To achieve this, we will simulate four times the response using Simulink model shown in Figure 5.3 at four disturbance frequencies: 101, 200, 1000, 5000 [rad/s], and visually compare their behaviors, which, as it is shown in Figure 5.4, will be quite similar.

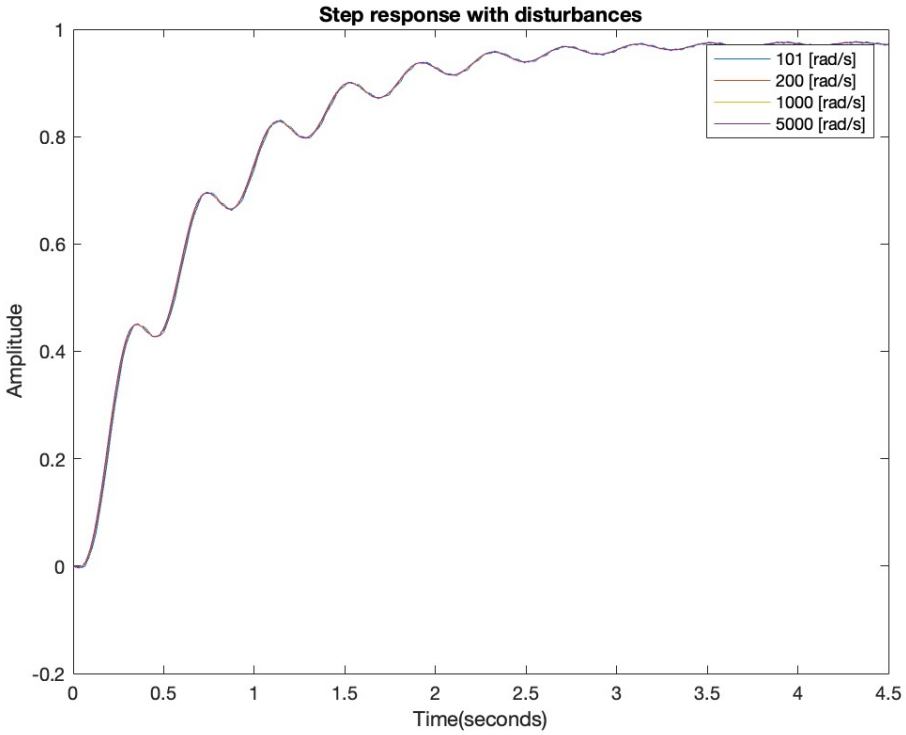

Figure 5.4: Multiple-frequency step response

After running the MATLAB code shown in Appendix B, the following step response infos for the step response with the disturbance at frequency $\omega = 101[rad/s]$ are provided:

RiseTime: 1.3099 [s]
SettlingTime (5%): 2.1873 [s]
Overshoot: 0.0814 %
Undershoot: 0.2745 %
Peak: 0.9777
PeakTime: 4.3211 [s]

We now want to compare the step response of the system affected by a measurement disturbance at frequency $\omega = 101[rad/s]$ to that of the system without disturbances. The graphical comparison is shown in Figure 5.5:

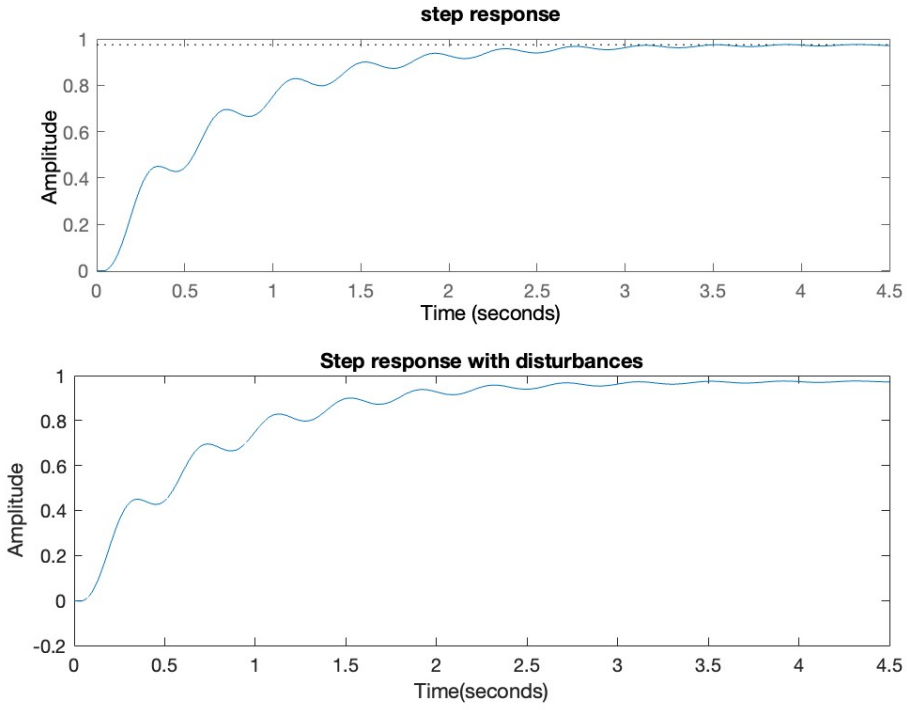

Figure 5.5: Graphical comparison

The differences in the main parameters of the closed-loop system step response with and without disturbances are:

rise.time.diff = 3.3627e-04 [s]
settling.time.diff = 0.0206 [s]
overshoot.diff = -0.0102%
undershoot.diff = 0.0098%
peak.diff = 0.0020

In conclusion, the analysis reveals that the system response to disturbances at frequencies larger than $101[rad/s]$ is very similar to the response of the system in absence of disturbances. This indicates that high-frequency disturbances have minimal impact on the overall system performance, thereby validating the robustness of the controlled system under such conditions.

Appendix A

Sensitivity to parametric variations

Let $G(s,\alpha), \alpha \in I$, where I is an appropriate interval, be a parametric description of a process with nominal value $G(s,\alpha_0)$, for a suitable $\alpha_0 \in I$.
To this set of processes corresponds a family of closed-loop systems $W(s,\alpha), \alpha \in I$.
These systems are derived from the preceding ones through the unitary feedback of $\tilde{G}(s) = G(s)C(s)$, where $C(s)$ is exempt from parametric variations, indicating that it remains constant with respect to α.
Now, let's define the **sensitivity function of the frequency response of the process** $G(s)$ as follows:

$$S_G = S_G(j\omega,\alpha) \coloneqq \frac{\partial G(j\omega,\alpha)}{\partial \alpha} \cdot \frac{1}{G(j\omega,\alpha)}$$

and the **sensitivity function of the frequency response of the closed-loop process** $W(s)$ as follows:

$$S_W = S_W(j\omega,\alpha) \coloneqq \frac{\partial W(j\omega,\alpha)}{\partial \alpha} \cdot \frac{1}{W(j\omega,\alpha)}.$$

Since it holds:

$$\frac{\partial W}{\partial \alpha} \cdot \frac{1}{W} = \frac{\partial(\frac{CG}{1+CG})}{\partial \alpha} \cdot \frac{1+CG}{CG} = \frac{\partial G}{\partial \alpha} \cdot \frac{1}{G} \cdot \frac{1}{1+CG}$$

it follows that:

$$S_W = \frac{1}{1+CG} \cdot S_G$$

This formula is of great importance because it relates S_G and S_W, allowing us to understand which control strategy we can adopt in order to minimize S_W over a range of frequencies ω.

Appendix B

MATLAB code

```
%% Initialization
clc
clear all
close all

%% Parameters

Ke = -371.6; % evans gain
K=1; % initialization of the proportional gain

%% Transfer function

s = tf('s');

%   define the system
sysG = Ke * ((s - 47.2) * (s + 47.2))/(s^2 + 3.329 *
   s + 248);

%   save numerator and denominator coefficients
   separately
numG = sysG.Numerator;
denG = sysG.Denominator;

%   save poles and zeros separately
pG = pole(sysG);
zG = zero(sysG);

sysGzpk = zpk(sysG);

%% Simulink model of Proportional feedback
```

```
open_system("Proportional");

%% Negative root locus

figure;
rlocus(sysG);
title("Negative rLocus of the closed-loop system");
xlabel('Real');
ylabel('Imaginary');

%   save margin values of negative rLocus
kcN = margin(sysG);

%% Positive root locus

figure;
rlocus(-sysG);
title("Positive rLocus of the clodes-loop system");
xlabel('Real');
ylabel('Imaginary');

%   save margin values of positive rLocus
kcP = margin(-sysG);

%% Bode plot

figure;
bode(sysG)
title("Bode Diagram");

%% Nyquist plot

%   negative feedback
figure;
nyquist(sysG)
hold on

%   mark critical point
plot(-1, 0, '.', 'MarkerSize', 30,'DisplayName',"
   Critical Point", "Color","red");
hold on

%   mark intersections with real axis
plot(-370.37, 0, '.', 'MarkerSize', 20,'DisplayName'
```

```
   ,"(-370.37,0)", "Color","black");
hold on
plot(3333.333, 0, '.', 'MarkerSize', 20,'DisplayName'
   ,"(3333.33,0)", "Color","black");
hold on

legend("G(s)","Critical Point","(-370.37,0)
   ","(3333.33,0)");
title("Negative feedback");

%% Controlled system

%   proportional C1
K = 0.009;
sysC1 = K;
figure;
bode(sysG * sysC1, {0.06,1000})
title("Bode with proportional controller");
grid on

%   C1 and C2
sysC = (0.0116) / (27*s + 1);
sysCG = sysC * sysG;
sysCGzpk = zpk(sysCG);

%   closed loop transfer function
sysW = minreal((sysC * sysG) / (1 + sysG * sysC ));
sysWzpk = zpk(sysW);

%   plot of Bode diagram of the controlled system
figure;
bode(sysCG)
grid on
title("Bode diagram of controlled system");

[Gm,Pm,Wcg,Wa]=margin(sysCG);

%% Simulink model of Controlled system

open_system("Controlled");

%% Step response

figure;
```

```
title("step response of open loop system");
step(sysG,6)

%   closed chain with simulink
open_system("Controlled");
set_param('Controlled', ...
    'SolverType', 'Variable-step', ...
    'Solver', 'ode45', ...
    'StopTime', '6');
sim('Controlled');

%   step response with CST
figure;
step(sysW,6)
title("step response");

%   step response info
stepinfos = stepinfo(sysW, 'SettlingTimeThreshold',
   0.05); %settling time 5%
stepinfos

%% Step response of the system with disturbances

open_system("Disturbances");

omega_hf = 101;  %[rad/s]

%   response analysis with simulink
open_system("Disturbances");
set_param('Disturbances', ...
    'SolverType', 'Variable-step', ...
    'Solver', 'ode45', ...
    'StopTime', '6');
sim('Disturbances');

%   now we want to get step infos of step response
   with disturbances
yd = ans.yout;
step_data_time_table = yd.extractTimetable;

%   seconds is used to extract a double array from a
   "duration" data type
step_data_time = seconds(step_data_time_table.Time);
step_data_data = step_data_time_table.Y_d;
```

```
%   plot of the response
figure;
plot(step_data_time, step_data_data);
title("Step response with disturbances");

%   step response info
stepinfos_dist = stepinfo(step_data_data,
   step_data_time, 'SettlingTimeThreshold', 0.05); %
   settling time 5%
stepinfos_dist

%% Comparison with step response without disturbances

%   graphic comparison
figure;
subplot(2,1,1);
step(sysW,4.5);
title("step response");

subplot(2,1,2);
plot(step_data_time, step_data_data);
xlabel("Time(seconds)");
ylabel("Amplitude");
title("Step response with disturbances");

%   numerical comparison
rise_time_diff = stepinfos_dist.RiseTime - stepinfos.
   RiseTime;
transient_time_diff = stepinfos_dist.TransientTime-
   stepinfos.TransientTime;
settling_time_diff = stepinfos_dist.SettlingTime -
   stepinfos.SettlingTime;
overshoot_diff = stepinfos_dist.Overshoot - stepinfos
   .Overshoot;
undershoot_diff = stepinfos_dist.Undershoot -
   stepinfos.Undershoot;
peak_diff = stepinfos_dist.Peak - stepinfos.Peak;

%   print of numerical comparison
rise_time_diff
transient_time_diff
settling_time_diff
overshoot_diff
undershoot_diff
```

```
peak_diff

%% Plot of mutiple step response with disturbances

%   decrease simulation time to 4.5 s

open_system("Disturbances");
set_param('Disturbances', ...
    'SolverType', 'Variable-step', ...
    'Solver', 'ode45', ...
    'StopTime', '4.5');

%   101 [rad/s]
omega_hf = 101;
sim('Disturbances');
yd = ans.yout;
step_data_time_table = yd.extractTimetable;
step_data_time = seconds(step_data_time_table.Time);
step_data_data = step_data_time_table.Y_d;

%   create the figure
figure;
plot(step_data_time, step_data_data,'DisplayName'
   ,"101 [rad/s]");
xlabel("Time(seconds)");
ylabel("Amplitude");
title("Step response with disturbances");

hold on

%   200 [rad/s]
omega_hf = 200;
sim('Disturbances');
yd = ans.yout;
step_data_time_table = yd.extractTimetable;
step_data_time = seconds(step_data_time_table.Time);
step_data_data = step_data_time_table.Y_d;
plot(step_data_time, step_data_data,'DisplayName'
   ,"200 [rad/s]");

hold on

%   1000 [rad/s]
omega_hf = 1000;
```

```
sim('Disturbances');
yd = ans.yout;
step_data_time_table = yd.extractTimetable;
step_data_time = seconds(step_data_time_table.Time);
step_data_data = step_data_time_table.Y_d;
plot(step_data_time, step_data_data,'DisplayName'
   ,"1000 [rad/s]");

%   5000 [rad/s]
omega_hf = 5000;
sim('Disturbances');
yd = ans.yout;
step_data_time_table = yd.extractTimetable;
step_data_time = seconds(step_data_time_table.Time);
step_data_data = step_data_time_table.Y_d;
plot(step_data_time, step_data_data,'DisplayName'
   ,"5000 [rad/s]");

legend("101 [rad/s]","200 [rad/s]","1000 [rad/s
   ]","5000 [rad/s]");
```

[0]All the Simulink block scheme are shown in the thesis

Bibliography

[1] Mauro Bisiacco, Maria Elena Valcher, *Controlli automatici II edizione*, "... tutto quello che avreste voluto sapere a riguardo ma non avete mai osato chiedere", Libreria Progetto Padova, 2015

[2] Mauro Bisiacco, Gianluigi Pillonetto, *Sistemi e Modelli*, Esculapio, 2017

[3] MWilliam J Palm III, *Introduction to MATLAB for Engineers*, McGraw-Hill Education, 2010

[4] ESA website: `https://www.esa.int/Enabling_Support/Space_Transportation/Launch_vehicles/Ariane_5`

[5] ESA website: `https://www.esa.int/Enabling_Support/Space_Transportation/Launch_vehicles/Ariane_5_ECA`

[6] ARIANESPACE website: `https://www.arianespace.com/vehicle/ariane-5/`